

# Direct Measurement of Ultrafast Carbon–Carbon Cleavage Rates via the Subpicosecond Charge-Transfer Activation of Pinacols

T. M. Bockman, S. M. Hubig, and J. K. Kochi\*

Contribution from the Chemistry Department, University of Houston, Houston, Texas 77204-5641

Received January 9, 1998

**Abstract:** Highly transient (benzpinacol) cation radicals ( $D_2^{+\bullet}$ ) and their ultrafast mesolytic fragmentations to the diarylhydroxymethyl radical ( $D^\bullet$ ) and cation ( $D^+$ ) are directly observed on the early picosecond time scale upon the charge-transfer photoactivation of the intermolecular donor–acceptor complexes of pinacol donors with methyl viologen. Ultrashort lifetimes of the cation radicals with  $\tau \approx 10$  ps obtain (for the first time) from quantitative kinetics analysis of the time-resolved spectroscopic results. These rapid C–C bond scissions successfully compete with back-electron transfer, which normally predominates on this time scale, and lead to exceptionally high efficiencies for the oxidative fragmentation of pinacols.

## Introduction

The unusually facile cleavage of benzpinacols to afford quantitative yields of various benzophenones in the presence of organic and inorganic oxidants<sup>1,2</sup> has been attributed to a labile intermediate—the pinacol cation radical<sup>3</sup> prone to mesolytic fragmentation.<sup>4</sup> However, relatively little quantitative information is available on the rate of this process, and the direct and unambiguous observation of the cleavage remains an experimental challenge. In this study, we demonstrate how the methodology that we previously employed to determine the rates of ultrafast reactions<sup>5</sup> can be utilized (a) to unambiguously identify the reactive intermediate and (b) to quantitatively measure its cleavage rate. The time-resolved fs spectroscopic method exploits charge-transfer activation to effect the instantaneous oxidation<sup>6</sup> on the subpicosecond time scale of the different pinacols identified in Chart 1. As such, this unique approach allows us now to determine the ultrafast rate constants for the C–C scission of transient pinacol cation radicals with

(1) (a) Penn, J. H.; Duncan, J. H. *J. Org. Chem.* **1993**, *58*, 2003. (b) Han, D. S.; Shine, H. J. *J. Org. Chem.* **1996**, *61*, 3977. (c) Lopez, L.; Mele, G.; Mazzeo, C. *J. Chem. Soc., Perkin Trans. 1* **1994**, 779.

(2) For a general review of oxidative cleavages of pinacols, see: House, H. O. *Modern Synthetic Reactions*, 2nd ed.; Benjamin: New York, 1972; p 353f.

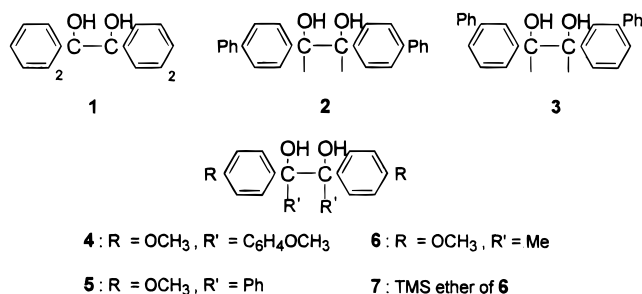
(3) (a) Reichel, L. W.; Griffin, G. W.; Muller, A. J.; Das, P. K.; Ege, S. N. *Can. J. Chem.* **1984**, *62*, 424. (b) Davis, H. F.; Das, P. K.; Reichel, L. W.; Griffin, G. W. *J. Am. Chem. Soc.* **1984**, *106*, 6968. (c) Chen, L.; Farahat, M. S.; Gaillard, E. R.; Farid, S.; Whitten, D. G. *J. Photochem. Photobiol. A* **1996**, *95*, 21. (d) Perrier, S.; Sankararaman, S.; Kochi, J. K. *J. Chem. Soc., Perkin Trans. 2* **1993**, 825. (e) Sankararaman, S.; Kochi, J. K. *J. Chem. Soc., Chem. Commun.* **1989**, 1800. (f) Albini, A.; Spreti, S. *J. Chem. Soc., Perkin Trans. 2* **1987**, 1175.

(4) (a) Maslak, P. *Top. Curr. Chem.* **1993**, *168*, 1. (b) Maslak, P.; Chapman, W. H., Jr. *J. Org. Chem.* **1996**, *61*, 2647. (c) Wayner, D. D. M.; Parker, V. D. *Acc. Chem. Res.* **1993**, *26*, 287.

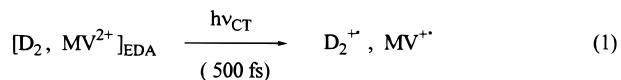
(5) (a) Hubig, S. M.; Bockman, T. M.; Kochi, J. K. *J. Am. Chem. Soc.* **1996**, *118*, 3842. (b) Bockman, T. M.; Hubig, S. M.; Kochi, J. K. *J. Org. Chem.* **1997**, *62*, 2210. (c) Bockman, T. M.; Hubig, S. M.; Kochi, J. K. *J. Am. Chem. Soc.* **1996**, *118*, 4502.

(6) Charge-transfer excitation of electron donor–acceptor complexes effects the transfer of an electron from the donor to the acceptor in less than 500 fs to produce the donor cation radical in the ground state. See: Wynne, K.; Galli, C.; Hochstrasser, R. M. *J. Chem. Phys.* **1994**, *100*, 4797. Thus the CT excited state (as the precursor to the ion-radical pair) must have a very short lifetime, and it is not chemically significant on the picosecond time scale.

Chart 1. Pinacol Donors ( $D_2$ )



lifetimes of  $\tau < 10$  ps by direct kinetic measurements as follows: The pinacols in Chart 1 form donor–acceptor complexes with electron-poor substrates such as quinones, cyanoarenes, and pyridinium cations.<sup>3d,e</sup> Charge-transfer activation of the EDA complex effects the instantaneous transfer of an electron from donor to acceptor, and thus generates the pinacol cation radical on a time scale that is rapid compared to its cleavage.<sup>6</sup> Time-resolved spectroscopy is then utilized to observe and quantify the ultrafast follow-up reactions. As the reactive acceptor in this reaction, we choose the methyl viologen dication (4,4′-dimethyl-1,1′-bipyridinium) owing to its well-defined (redox) spectral changes. Charge-transfer (CT) excitation of the electron donor–acceptor or EDA complexes of various pinacolic donors ( $D_2$ ) with methyl viologen ( $MV^{2+}$ ) leads to the ultrafast co-generation of the cation radical ( $D_2^{+\bullet}$ ) and the reduced acceptor ( $MV^{\bullet+}$ ) upon the 200-fs laser excitation, i.e.



The subsequent disappearance of the pinacol cation radical and the reduced methyl viologen may then be observed spectroscopically on the early picosecond time scale.

## Results and Discussion

**Spectral Identification of Highly Transient (Pinacol) Cation Radicals.** Charge-transfer excitation of the EDA

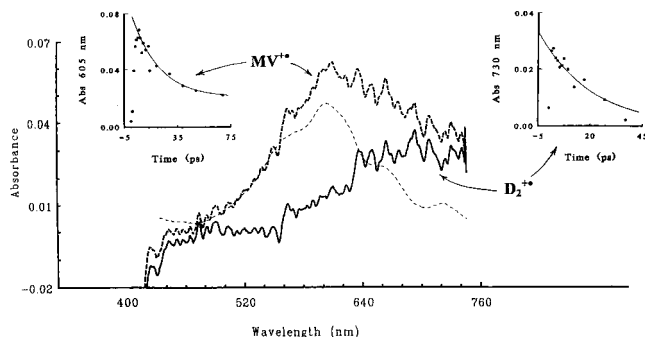


**Figure 1.** Transient absorption spectrum (---) observed upon the 400-nm (200-fs) laser excitation of the EDA complex of  $MV^{2+}$  and pinacol **2** in acetonitrile, and the absorption band of  $2^{+•}$  (—) obtained by spectral subtraction of the authentic absorption of  $MV^{+•}$  (···). The insets show the decays of the 605- and 730-nm absorptions of  $MV^{+•}$  and  $2^{+•}$ , respectively, fitted to first-order kinetics (solid lines) both with  $k = 5 \times 10^{10} \text{ s}^{-1}$ .

complex of pinacol **2** with  $MV^{2+}$  in acetonitrile generated (within 500 fs) a transient spectrum with a broad absorption centered at 605 nm and extending beyond 750 nm (see Figure 1). Digital subtraction of the authentic spectrum of the reduced methyl viologen ( $MV^{+•}$ )<sup>7</sup> in Figure 1 revealed an absorption band centered at 730 nm, which was readily assigned to the cation radical of **2**.<sup>8</sup> Quantitative comparison of the absorption bands of  $MV^{+•}$  and  $2^{+•}$  initially upon laser excitation established the requisite 1:1 stoichiometry for the production of the two ion radicals as described in eq 1.<sup>9</sup> The assignment of the 730-nm band to the pinacol cation radical,  $2^{+•}$  was further confirmed by its independent generation via the charge-transfer irradiation of the EDA complex of **2** with dimethyl dicyanofumarate.<sup>10</sup> In this experiment, the band of the cation radical ( $2^{+•}$ ) was observed without interference from the absorptions of the reduced acceptor, which was transparent in this spectral region.

The absorbances of  $D_2^{+•}$  at 730 nm and  $MV^{+•}$  at 605 nm both decreased concomitantly on the picosecond time scale with identical (first-order) rate constants of  $k = (5 \pm 0.5) \times 10^{10} \text{ s}^{-1}$ . Whereas the absorption band of  $D_2^{+•}$  fully decayed to the spectral baseline within 50 ps, the simultaneous decay of  $MV^{+•}$  resulted in a residual intensity at 50 ps of ~15%, as shown in the insets of Figure 1; and this absorption remained unchanged over nanoseconds. The same kinetics was observed upon the subpicosecond excitation of the EDA complexes of the pinacols **4–7** in Chart 1—i.e., the complete decay of the cation radical  $D_2^{+•}$ <sup>11</sup> in less than 30 ps and the partial decay of  $MV^{+•}$  on the same time scale to the residual absorbances ( $R$ ) listed in Table 1. In all cases, the kinetic evaluation of the decays of both ion radicals afforded identical (first-order) rate constants, which permitted us to select the common spectral peak at  $\lambda_{\text{max}} = 605 \text{ nm}$  as the general monitoring wavelength for the decay of all the pinacol cation radicals in Chart 1.

**Table 1.** Rates of Carbon–Carbon Scission of Pinacol Cation Radicals as Transient Intermediates in the Charge-Transfer Activation of EDA Complexes<sup>a</sup>

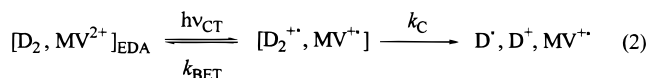
pinacol <sup>b</sup>	$k^c$ ( $10^{10} \text{ s}^{-1}$ )	$R^d$	$k_{\text{C-C}}^{e,g}$ ( $10^{10} \text{ s}^{-1}$ )	$k_{\text{BET}}^{f,g}$ ( $10^{10} \text{ s}^{-1}$ )
<b>1</b>	6.0	0.30	1.4 <sup>h</sup>	4.6 <sup>h</sup>
<b>2</b>	4.8	0.11	0.5	4.3
<b>3</b>	3.8	0.09	0.3	3.5
<b>4</b>	23	0.35	8.0	15
<b>5</b>	41	0.12	4.9	36
<b>6</b>	50	0.11	5.3	44
<b>7</b>	38	0.16	6.0	32

<sup>a</sup> In acetonitrile at 25 °C. <sup>b</sup> Identified in Chart 1. <sup>c</sup> Observed rate constant for the decay of the ion radicals  $D_2^{+•}$  and  $MV^{+•}$ . <sup>d</sup> Relative amounts of residual  $MV^{+•}$  after the complete decay of  $D_2^{+•}$  (see text). <sup>e</sup> Rate constant for C–C bond cleavage in eq 2. <sup>f</sup> Rate constant for back electron transfer in eq 2. <sup>g</sup> Calculated from the values of  $R$  and  $k$  (see ref 18), unless otherwise indicated. <sup>h</sup> Obtained from the digital simulation in Figure 3.

### Direct Observation of the Ultrafast (Pinacol) Cleavage.

The predominant pathway for the decay of ion radicals generated by charge-transfer excitation of EDA complexes is back-electron transfer within the initial ion-radical pair.<sup>12</sup> Since complete back-electron transfer restores the original starting components of the EDA complex, it results in a zero baseline of the transient spectra. On the other hand, the observation of residual absorbances ( $R$ ) pointed to a more complex reaction scheme in which at least one other decay pathway competed with the ubiquitous back-electron transfer.<sup>13</sup> As such, we now identify the mesolytic cleavage ( $k_{\text{C}}$ ) of the pinacol cation radical  $D_2^{+•}$  into its fragments  $D^•$  and  $D^+$  as the additional decay pathway that generates residual amounts of reduced methyl viologen in accord with reaction 2 (Scheme 1). To establish the validity of the bond scission ( $k_{\text{C}}$ ) in Scheme 1, we utilized time-resolved

### Scheme 1



spectroscopy to detect the characteristic cleavage product  $D^•$  of the pinacol cation radicals. Most importantly, the formation of  $D^•$  on the picosecond time scale was simultaneous with the decays of  $D_2^{+•}$  and  $MV^{+•}$ . For example, charge-transfer excitation of the EDA complex of pinacol **1** with  $MV^{2+}$  in acetonitrile led initially to a transient absorption spectrum that was identical with the authentic spectrum of reduced methyl viologen<sup>7</sup> (see Figure 2A). At later times (50–200 ps after excitation), additional absorptions progressively grew in on the blue edge of the 605-nm band of  $MV^{+•}$  (see Figure 2B). Digital subtraction of the authentic spectrum of  $MV^{+•}$ <sup>7</sup> from the composite spectrum in Figure 2B revealed the new absorption band centered at 535 nm, which was readily assigned to the diphenylhydroxymethyl radical.<sup>14</sup> This radical ( $D^•$ ) was clearly

(7) (a) Watanabe, T.; Honda, K. *J. Phys. Chem.* **1982**, *86*, 2617. (b) Bockman, T. M.; Kochi, J. K. *J. Org. Chem.* **1990**, *55*, 4127.

(8) The absorption spectra of  $2^{+•}$  and  $3^{+•}$  are essentially the same as those of the cation radicals of the methylbiphenyls, which were generated independently by CT excitation of their EDA complex with tetracyanobenzene. Compare: Ojima, S.; Miyasaka, H.; Mataga, N. *J. Phys. Chem.* **1990**, *94*, 7534.

(9) Based on  $\epsilon_{605} = 14\,100 \text{ M}^{-1} \text{ cm}^{-1}$  as the extinction coefficient of reduced methyl viologen at 605 nm.<sup>7</sup> The extinction coefficient of  $2^{+•}$  at 730 nm is taken as that of the 4-methylbiphenyl cation radical ( $\epsilon_{730} \approx 10\,000 \text{ M}^{-1} \text{ cm}^{-1}$ ).<sup>8</sup>

(10) Dimethyl dicyanofumarate has been identified as a versatile electron acceptor in thermal electron-transfer reactions. See: Gotoh, T.; Padias, A. B.; Hall, H. K., Jr. *J. Am. Chem. Soc.* **1986**, *108*, 4920.

(11) The cation radicals of the methoxy-substituted pinacols absorb in the same wavelength region (450–470 nm) as the anisole cation radical. See: Takamaku, S.; Komitsu, S.; Toki, S. *Radiat. Phys. Chem.* **1989**, *34*, 553.

(12) See: (a) Asahi, T.; Mataga, N. *J. Phys. Chem.* **1989**, *93*, 6575. (b) Asahi, T.; Mataga, N. *J. Phys. Chem.* **1991**, *95*, 1956. (c) Peters, K. S. *Adv. Electron-Transfer Chem.* **1994**, *4*, 27. (d) Hilinski, E. F.; Masnovi, J. M.; Kochi, J. K.; Rentzepis, P. M. *J. Am. Chem. Soc.*, **1984**, *106*, 8071. (e) Fox, M. A. *Adv. Photochem.* **1986**, *13*, 237.

(13) For examples, see: Bockman et al. in ref 5b and Masnovi et al. (Masnovi, J. M.; Kochi, J. K.; Hilinski, E. F.; Rentzepis, P. M. *J. Am. Chem. Soc.* **1986**, *108*, 1126). See also Ojima et al. in ref 8.

(14) See: Hayon, E.; Ibat, T.; Lichtin, N. N.; Simic, M. *J. Phys. Chem.* **1972**, *76*, 2072, and ref 5b.

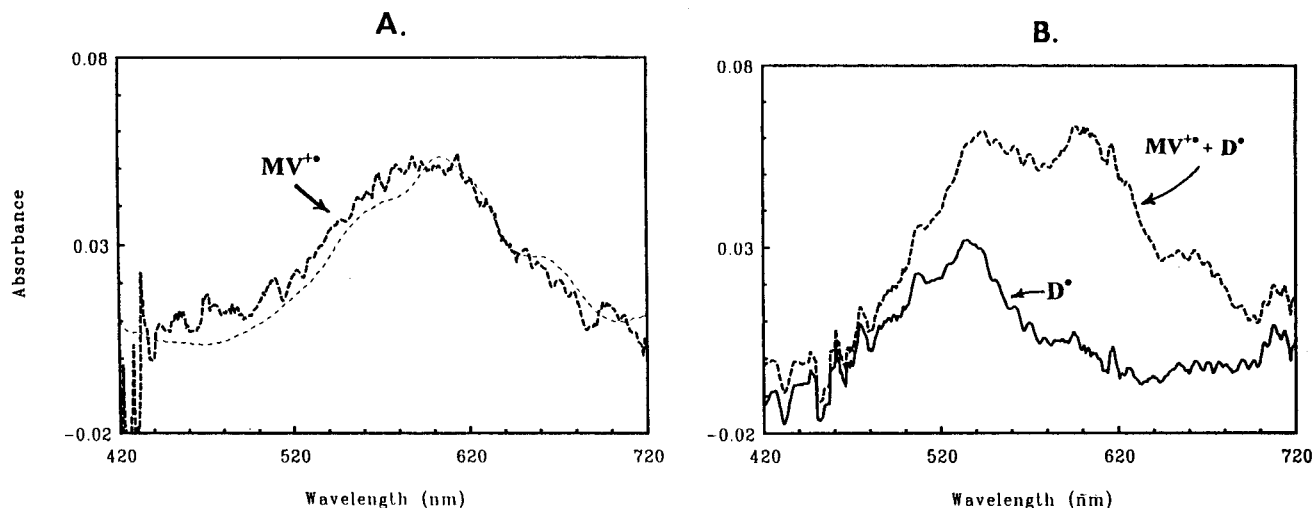
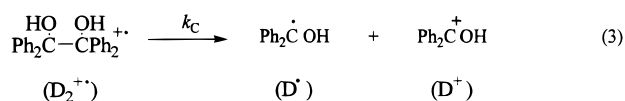


**Figure 2.** (A) Transient absorption spectrum of only  $MV^{2+}$  (---) obtained at 20 ps following the 355-nm (25-ps) laser excitation of the EDA complex of  $MV^{2+}$  and pinacol **1** in acetonitrile in comparison with authentic  $MV^{2+}$  (—). (B) Composite spectrum (---) obtained 200 ps later, and spectrum of  $D^{\bullet}$  (—) obtained by subtraction of the absorption band of  $MV^{2+}$  (shown in part A).

the direct product of the mesolytic fragmentation of the benzpinacol cation radical ( $D_2^{+\bullet}$ ) according to eq 3:



The characteristic absorption band of the radical  $D^{\bullet}$  with  $\lambda_{\text{max}} = 535$  nm was also observed upon charge-transfer excitation of the EDA complexes of **1** with other acceptors such as 1,2,4,5-tetracyanobenzene (TC) and 4-cyano-*N*-methylpyridinium ( $CP^+$ ). For example, laser activation of the EDA complex [**1**, TC] gave rise on the early picosecond time scale to the spectral absorption bands of the same radical  $D^{\bullet}$  as well as the anion radical of the new acceptor  $TC^{\bullet-}$ .<sup>15</sup> The spectral absorption band of  $D^{\bullet}$  observed upon irradiation of the complex of **1** with the cationic acceptor  $CP^+$  was unencumbered by the absorption of the reduced neutral acceptor ( $CP^{\bullet}$ ), which does not absorb visible light.<sup>16</sup> In other words, the one-electron oxidation of benzpinacol with a variety of acceptors, including neutral (TC), monocationic ( $CP^+$ ), and dicationic ( $MV^{2+}$ ) types, always led to the same cleavage of the pinacol cation radical  $1^{+\bullet}$  (see eq 3).

**Picosecond Rates for the Carbon–Carbon Bond Cleavages.** Quantitative comparison of the absorption bands of  $D^{\bullet}$  and  $MV^{2+}$  indicated that the amount of reduced methyl viologen (residual after 200 ps) was equivalent to the amount of radical  $D^{\bullet}$  formed by the cleavage of the pinacol cation radical  $D_2^{+\bullet}$  within the same time span, and thus confirmed the stoichiometry in eq 2.<sup>17</sup> [Note that the diphenylhydroxymethyl cation ( $D^+$ ) does not absorb visible light.<sup>17b</sup>] Accordingly, the complex kinetics in Scheme 1 was digitally simulated by taking into account the finite rise time of the laser pulse ( $h\nu_{CT}$ ); and Figure 3 typically shows the kinetic profiles of both the cation radical  $MV^{2+}$  and the radical  $D^{\bullet}$ , calculated with the rate constants  $k_C = 1.4 \times 10^{10} \text{ s}^{-1}$  and  $k_{BET} = 4.6 \times 10^{10} \text{ s}^{-1}$ . The experimental

values for the transient absorptions of these species are superimposed in Figure 3, and the excellent agreement between the computer simulation and the experimental points confirms the kinetics formulation in Scheme 1. On the basis of this scheme, the absolute values of  $k_C$  and  $k_{BET}$  for all the pinacol donors were computed from the overall rate constants of the ion-radical decay ( $k$ ) and the residual ( $R$ ) amounts of  $MV^{2+}$  according to the equations  $R = k_C/(k_C + k_{BET})$  and  $k = k_C + k_{BET}$ ,<sup>18</sup> and the results are listed in Table 1.

**Enhanced Efficiency of Pinacolic Cleavage via Charge-Transfer Activation.** Charge-transfer photoactivation spontaneously generates  $D_2^{+\bullet}$  as the ion-radical pair within 500 fs, in accord with the Mulliken formulation in eq 1.<sup>6</sup> Previous investigations have shown that the initial photoinduced electron transfer ( $h\nu_{CT}$ ) is usually followed by an ultrafast reverse electron transfer ( $k_{BET}$ ) to regenerate the pinacol  $D_2$  as the ground-state EDA complex.<sup>12</sup> However, the persistence of the residual absorption of  $MV^{2+}$  in Figures 1 and 2 points to another process that must compete with the back-electron transfer. Since the formation of the radical  $D^{\bullet}$  as the direct product of C–C bond cleavage was observed *simultaneously* with the rise and partial decay of  $MV^{2+}$  in Figure 3, the fragmentation of the

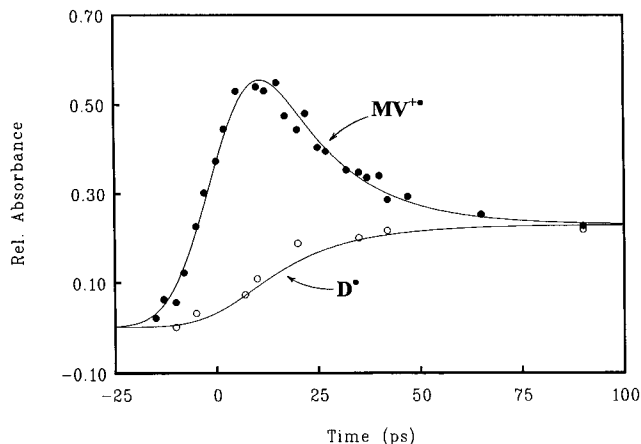


**Figure 3.** Formation and decay of  $MV^{2+}$  (●) and the formation of  $D^{\bullet}$  (○) upon excitation of  $[MV^{2+}, \mathbf{1}]$  presented in Figure 2. The solid lines correspond to the simulated changes of  $MV^{2+}$  and  $D^{\bullet}$  calculated according to the kinetics formulation in Scheme 1.

(15) Ojima, S.; Miyasaka, H.; Mataga, N. *J. Phys. Chem.* **1990**, *94*, 4147.

(16) Itoh, M.; Nagakura, S. *Bull. Chem. Soc. Jpn.* **1966**, *39*, 369.

(17) (a) The extinction coefficient of the ketyl radical is  $\epsilon_{535} = 5800 \text{ M}^{-1} \text{ cm}^{-1}$ .<sup>14</sup> For the extinction coefficient of the reduced methyl viologen, see ref 9. (b) Ireland, J. F.; Wyatt, P. A. H. *J. Chem. Soc., Faraday Trans. I* **1973**, *69*, 161.

(18) Asahi, T.; Ohkohchi, M.; Mataga, N. *J. Phys. Chem.* **1993**, *97*, 13132.

Chart 2

Pinacol	$\sigma$	$\log k_C$	$\log k_{\text{BET}}$	$k_C / k_{\text{BET}}$
3	+0.06	9.48	10.54	0.09
2	-0.01	9.70	10.63	0.12
6	-0.27	10.72	11.64	0.12
----- $\rho$		-3.8	-3.5	

pinacol cation radical ( $k_C$  in eq 3) must effectively compete with back-electron transfer in Scheme 1.

The magnitudes of the cleavage rate constants for the various pinacol donors in Table 1 are strikingly insensitive to the substituents (hydrogen, phenyl, or methoxy) on the phenyl rings. In particular, we note in Chart 2 that the structurally related series of pinacols **2**, **3**, and **6** follow a Hammett correlation, in which both  $\log k_C$  and  $\log k_{\text{BET}}$  decrease linearly with the  $\sigma$  constant. In other words, the mesolytic fragmentation and reverse electron transfer respond to substituent effects in precisely the same way, as quantitatively reflected in the values of the Hammett parameter,  $\rho = -3.8$  and  $-3.5$ , respectively. As a result, the overall efficiency of cleavage *vis a vis* back-electron transfer remained more or less the same with all substituents. The rather invariant ratio between  $k_C$  and  $k_{\text{BET}}$  for the various substituted pinacols in Table 1 thus accounts for the previously puzzling observation that the quantum yields are singularly independent of the substituents.<sup>3d</sup>

We believe that the positive trend in  $k_C$  with donor substituents relates mainly to the increasing stability of the fragmentation products,  $D^\bullet$  and  $D^+$ , especially the latter, as the substituent is changed.<sup>4b</sup> Indeed, the cleavages of *all* the pinacol cation radicals in Table 1 are ultrafast, with unimolecular rate constants in the range  $k_C = 10^{10}$ – $10^{11}$  s<sup>-1</sup> and activation energies of less than 5 kcal mol<sup>-1</sup>.<sup>19</sup> Thus the dissociation energy of the central carbon–carbon bond in the benzpinacol cation radical is reduced by about 35 kcal mol<sup>-1</sup> compared to that of the neutral pinacol prior to oxidation.<sup>20</sup> In fact, the fast rate constants ( $k_C$ ) which are comparable to those of the competing back-electron transfer ( $k_{\text{BET}}$ ) result in unusually high photochemical efficiencies for the charge-transfer activated cleavages of pinacols.<sup>21</sup> The high quantum yields are particularly noteworthy, since photochemistry via charge-transfer activation is commonly limited by the efficient (energy-wasting) back-electron transfer.<sup>22</sup>

**Ultrafast Cleavages That Obviate Ion-Pair Microdynamics.** The successful analysis of the transient (ps) spectral changes in Figure 3 derives from the remarkably straightforward mechanism in Scheme 1. As such, it is especially noteworthy that Scheme 1 is singularly devoid of other (physical) processes that are usually encountered in photoinduced (electron-transfer) microdynamics such as ion-pair dissociation/reassociation, solvation, intersystem crossing, etc.<sup>23</sup> To establish the limits to

(19) Estimated on the basis of the Eyring equation. See: Moore, J. W.; Pearson, R. G. *Kinetics and Mechanism*, 3rd ed.; Wiley: New York, 1981; p 173.

(20) The dissociation energies for the central C–C bonds in the neutral pinacols are taken as those of the corresponding dimethyl ethers (38–46 kcal mol<sup>-1</sup>). See: Birkhofer, H.; Beckhaus, H.-D.; Peters, K.; von Schnering, H.-G.; R uchardt, C. *Chem. Ber.* **1993**, *126*, 1693.

(21) Note that the subsequent oxidation of  $D^\bullet$  by  $MV^{2+}$  to complete the stoichiometry for the retopinacol reaction occurs by second-order kinetics and is too slow to be observed on the picosecond time scale.

(22) The photochemical quantum yields of CT-activated photoreactions are generally very low ( $<10^{-2}$ ). See, e.g.: Jones, G., II In *Photoinduced Electron Transfer: Part A*; Fox, M. A., Chanon, M., Eds.; Elsevier: Amsterdam, 1988; p 245.

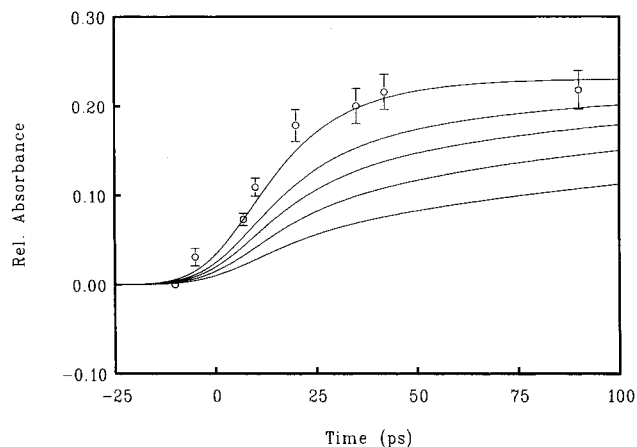
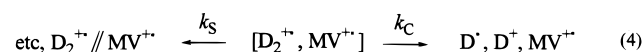


**Figure 4.** Comparison of the experimental data for the formation of the radical  $D^\bullet$  (O) with the computer simulations of its rise with varying values of the separation rate constant in eq 4 (see text). The solid lines (top to bottom) are simulated with values of  $k_S = 0, 4 \times 10^9, 6 \times 10^9, 8 \times 10^9$ , and  $10 \times 10^9$  s<sup>-1</sup>, and the error bars represent the experimental uncertainty of  $\pm 10\%$ .

which the latter may complicate the formulation in Scheme 1, let us consider the competition for the contact ion pair in Scheme 1 as:



where  $k_S$  represents the (composite) rate constant for all such (first-order) processes. Such a competition(s) is readily evaluated by the digital simulation of Scheme 1 as modified by the inclusion of  $k_S$  to convert the initial contact ion pair to a species that does not undergo back-electron transfer in the ps time domain. Importantly, kinetics analysis (as detailed in the Experimental Section) predicts a distinct time lag between the back-electron transfer (as monitored by the decay of  $MV^{+\bullet}$ ) and the cleavage (as monitored by the rise of  $D^\bullet$ ). Figure 4 shows that such a time lag is *not* observed, and we must conclude that  $k_S$  is more than a factor of 10 slower than the cleavage rate constant,  $k_C$ .<sup>24</sup> In other words, the mesolytic cleavage of pinacols not only competes with ultrafast back-electron transfer, but it clearly outruns all other ion-dynamical processes (such as solvent separation and recombination) that are generally involved in photoinduced electron transfers.<sup>25</sup> As a result, the elementary chemical steps of C–C bond cleavage and back-electron transfer of the ion-radical pair within its initial solvent cage stand alone from the usual (extramural) physicochemical processes of ion-pair relaxation, diffusion, and migration that complicate photoinduced electron transfers on longer time scales.

(23) See, e.g.: (a) Kavarnos, G. J.; Turro, N. J. *Chem. Rev.* **1986**, *86*, 401. (b) Gould, I. R.; Farid, S. *Acc. Chem. Res.* **1996**, *29*, 522. (c) Mauzerall, D. C. In *Photoinduced Electron Transfer: Part A*; Fox, M. A., Chanon, M., Eds.; Elsevier: Amsterdam, 1988; p 228.

(24) (a) Such a rate constant of  $k_S < 10^9$  s<sup>-1</sup> is consistent with simple diffusive separation of the ions in contact ion pairs. See: (b) Knibble, H.; Rehm, D.; Weller, A. *Ber. Bunsen-Ges. Phys. Chem.* **1968**, *72*, 257. (c) Ojima, S.; Miyasaka, H.; Mataga, N. *J. Phys. Chem.* **1990**, *94*, 7534. For the separation of cation–cation pairs, see: (d) Hubig, S. M. *J. Phys. Chem.* **1992**, *96*, 2903.

(25) Since the critical intermediate in CT photoactivation is the contact ion pair [ $D_2^{+\bullet}, MV^{+\bullet}$ ], the competing processes of back-electron transfer and C–C bond scission occur within the solvent cage, and do not involve solvent-separated or free species. However, such a formulation does not preclude the involvement of a variety of contact ion pairs (relaxed or unrelaxed) with different rates of back electron transfer and cleavage. It is notable, however, that the identical competition between cleavage and back ET governs the reactions of both positive-positive ion pairs [ $D_2^{+\bullet}, MV^{+\bullet}$ ], as well as oppositely charged ion pairs [ $D_2^{+\bullet}, TC^{-\bullet}$ ].

We hope that further studies on the femtosecond and picosecond time scales will bring to solution-phase chemistry the elegance and simplicity that characterize the dynamics in the gas phase.

## Summary and Conclusions

Charge-transfer (laser) excitation of the EDA complexes of various substituted benzpinacols with methyl viologen effects ultrafast cleavage of the pinacol, and time-resolved (fs/ps) spectroscopy offers the opportunity to quantitatively monitor the retropinacol reaction step by step. Scheme 1 presents carbon-carbon bond scission and back-electron transfer as the two dominant pathways for the decay of the pinacol cation radical, and the rate constants for both competing processes can thus be determined from the temporal decay of the transients. Direct kinetic measurements reveal for the first time a series of ultrafast ( $10^{10}$  to  $10^{11}$  s<sup>-1</sup>) cleavage rates of pinacol cation radical which can readily compete with back-electron transfer within the ion-radical pair. As a result, efficient pinacol cleavage can be achieved by simple photoactivation of the electron donor-acceptor complexes of pinacols with various acceptors.<sup>3d</sup>

## Experimental Section

**Materials.** Benzophenone (Aldrich) was recrystallized from ethanol before use. 4-Methoxyacetophenone, 4-methoxybenzophenone, 4,4'-dimethoxybenzophenone, 4-acetylbiphenyl, and 1,2,4,5-tetracyanobenzene (Aldrich) were used as received. Samarium diiodide was used in the form of a 0.1 M solution in tetrahydrofuran as supplied by Aldrich. The solvents acetonitrile and dichloromethane were spectrophotometric grade and used as received. Tetrahydrofuran was distilled from sodium and benzophenone under an inert argon atmosphere. Dimethyl dicyanofumarate was prepared by the method reported in the literature.<sup>26</sup>

**Synthesis of the pinacol donors.** The pinacols substituted with methyl groups on the bridge were synthesized by reductive coupling of the corresponding acetophenones, promoted by samarium diiodide, as follows. Under an inert atmosphere of argon, the acetophenone (0.01 mol) was dissolved or suspended in 50 mL of tetrahydrofuran at room temperature. A solution of samarium diiodide (100 mL; 0.1 M) in tetrahydrofuran was added through a stainless steel cannula by using a positive pressure of argon. The mixture was stirred magnetically as the dark blue-green solution became pale yellow in color. The mixture was stirred at room temperature for 2 h more, and 30 mL of saturated sodium bicarbonate was then added. The reaction mixture was filtered through a 5-cm pad of Celite and washed with a total of 200 mL of diethyl ether. The organic fraction of the filtrate was separated, and the aqueous layer was extracted with diethyl ether (3 × 50 mL). The combined organic layers were washed sequentially with 5% aqueous sodium bisulfite and water, and then dried with anhydrous magnesium sulfate. The solvent was removed by rotary evaporation, and the crude product was adsorbed on silica gel. The pinacols were isolated by chromatography on a silica gel column by using mixtures of hexane and ethyl acetate as eluants and were purified by recrystallization from the same solvent mixture. **2,3-Bis(4'-methoxyphenyl)-2,3-butanediol:** yield 60%, as a 3:1 mixture of *meso* and *dl* isomers.<sup>27</sup> <sup>1</sup>H NMR (CDCl<sub>3</sub>): *meso* isomer (CDCl<sub>3</sub>) δ 7.14 (m, 4H), 6.80 (m, 4H), 3.83 (s, 6H), 1.49 (s, 6H). *dl* isomer (CDCl<sub>3</sub>) δ 7.16 (m, 4H), 6.76 (m, 4H), 3.80 (m, 6H), 2.2 (s, OH), 1.57 (s, 6H). **2,3-Bis-(4'-biphenyl) 2,3-butanediol:** yield 48% as a mixture of isomers. <sup>1</sup>H NMR (CDCl<sub>3</sub>): δ 7.78–7.28 (m, 18H), 1.67 (s, major isomer), 1.61 (s, minor isomer). **2,3-bis-(3'-biphenyl) 2,3-butanediol:** yield 20% as a single isomer. <sup>1</sup>H NMR (CDCl<sub>3</sub>): δ 7.50–7.28 (m, 18 H), 2.7 (s, 2H), 1.72 (s, 6H). The other pinacols were synthesized by the photoreduction of the corresponding benzophenones in isopropyl alcohol and were recrystallized from the same solvent. **1,1,2,2-Tetrakis-(4'-methoxyphenyl)-1,2-ethanediol:**<sup>28</sup> yield 20%; mp 180–182 °C. **1,1,2,2-Tetraphenyl-**

**1,2-ethanediol (benzpinacol):**<sup>29</sup> yield 78%, mp 187–188 °C. **1,2-Diphenyl-1,2-bis(4'-methoxyphenyl)-1,2-ethanediol:** yield 64% as a 1:1 mixture of isomers. <sup>1</sup>H NMR (CDCl<sub>3</sub>): δ 7.34 (m, 4H), 7.20 (m, 10H), 6.73 (m, 4H), 3.83 (s, 3H, isomer 1), 3.81 (s, 3H, isomer 2). The bis-trimethylsilyl ether, 2,3-bis-(4'-methoxyphenyl)-2,3-bis(trimethylsilyloxy)butane, was prepared by the reductive coupling of 4'-methoxyacetophenone with magnesium in hexamethylphosphoric triamide in the presence of chlorotrimethylsilane and was recrystallized as a single isomer from ethyl acetate and hexane.<sup>30</sup> <sup>1</sup>H NMR (CDCl<sub>3</sub>): δ 7.42 (m, 4H), 6.83 (m, 4H), 3.83 (s, 6H), 1.37 (s, 6H), 0.02 (s, 18H).

**Instrumentation.** The time-resolved spectroscopic measurements on the femtosecond and on the picosecond and nanosecond/microsecond time scales were acquired with laser spectroscopic systems that have been described previously.<sup>31</sup> <sup>1</sup>H and <sup>13</sup>C NMR spectra were recorded on a General Electric QE-300 NMR spectrometer and the chemical shifts are reported in ppm units downfield from tetramethylsilane. Melting points were recorded on a Mel-Temp apparatus and are uncorrected.

**Preparation of Samples for Time-Resolved Spectroscopy.** Solutions of the acceptors (0.04–0.5 M) and the pinacols (0.02–0.1 M) were prepared in acetonitrile for experiments on the femtosecond and on the picosecond time scales. Preliminary experiments indicated that laser irradiation generated large amounts of reduced acceptor, which interfered with the time-resolved measurements. Accordingly, the solutions were prepared in the open air atmosphere and were not degassed. Since the problem was particularly acute for the methyl viologen acceptor, it necessitated the solutions to be saturated with pure oxygen prior to spectroscopic measurements. The sample cell for the experiments with methyl viologen was a 1.0 cm quartz flow cell, and the sample solution was circulated with a Labline 5514 peristaltic pump to minimize problems arising from secondary photolysis of the products. Connections were made with Teflon and Fluoran tubing. The UV-vis spectra of the circulating solution were acquired before and after laser photolysis to ensure that no significant thermal or photochemical changes had occurred. The experiments with the other acceptors were carried out under nonflow conditions, and the sample was changed after each spectral acquisition to minimize problems of secondary photolysis. The samples were further checked by acquisition of spectra prior to the laser pulse, and the solution was changed if there was any indication of long-lived spectral features. Each spectrum was an average of 100 laser shots, and the spectra were smoothed with a 5-point adaptive smoothing routine.

The yields of residual reduced methyl viologen (*R*) upon excitation of the pinacol/MV<sup>2+</sup> complexes were measured by the method of transient actinometry described earlier.<sup>5b</sup> Solutions of methyl viologen ditriflate and the pinacol donor were prepared in a 1-cm quartz cuvette equipped with a Teflon valve and the absorbance at 355 nm was adjusted to match that of the actinometer solution. The solutions were then degassed by four freeze-pump-thaw cycles. The transient absorbance of MV<sup>•+</sup> was determined at 605 nm. The trace was linearly extrapolated to zero time to ensure that the secondary formation of the reduced acceptor, which was formed on the 50–500 ns time scale, was not included. The values of *R* so obtained did not vary with the energy of the laser pulse (5–25 mJ).

**Kinetics Analysis of the Formation and Decay of the Radical Pairs.** The absorbance of reduced methyl viologen on the picosecond time scale was analyzed as described earlier,<sup>5b</sup> except that the temporal pulse shape of the laser was simulated as a Gaussian ( $I_{\text{abs}} = \exp[-(t/\tau)^2]$ ).<sup>32</sup> A value of  $\tau = 12$  ps (corresponding to a 21-ps pulse width) was obtained by simulating the rise of the signal of reduced methyl viologen in Figure 3. The kinetics in Scheme 1 were numerically integrated with a Microsoft QBASIC program that calculated the

(29) Bachmann, W. E. In *Organic Syntheses*; Blatt, A. H., Ed.; Wiley: New York, 1943; Collect. Vol. II, p 71.

(30) Perrier, S. Ph.D. Thesis, University of Houston, 1995.

(31) (a) For the flash photolysis experiments, a Ti:sapphire laser system (200 fs, 400 nm, 2 mJ)<sup>5b</sup> and a Nd: YAG laser (25 ps, 355 nm, 10 mJ)<sup>31b</sup> were used. (b) Bockman, T. M.; Kochi, J. K. *J. Chem. Soc., Perkin Trans. 2* **1996**, 1633.

(32) Peters, K. S.; Li, B. *J. Phys. Chem.* **1994**, 98, 401.

(26) Ireland, C. J.; Jones, K.; Pizey, J. S.; Johnson, S. *Synthet. Commun.* **1976**, 6, 185.

(27) Sisido, K.; Nozaki, H. *J. Am. Chem. Soc.* **1948**, 70, 778.

(28) Depovere, P.; Devis, R. *Bull. Soc. Chim. Fr.* **1968**, 6, 2470.

integrals by means of the trapezoid rule. The temporal step size was 1 ps and the data were plotted with use of the program Slidewrite Plus. The best fit for  $k$  in Figure 3 was obtained by overlaying the experimental data points with the simulated rises and decays for various values of  $k$ . A fixed value of  $k_{CC} = 0.3k_{BET}$  was used to ensure the agreement of the residual absorbance of  $MV^{+\bullet}$  with the value of  $R = 0.3$  for the methyl viologen/benzpinacol complex determined on the nanosecond time scale.

The possible incursion of reactions other than C–C bond cleavage (which might give rise to residual ion radicals) was tested by digital simulation. Scheme 1 was modified as follows: A reaction step, with rate constant  $k_S$ , was added. This step converted the contact ion-radical pair to an “inactive” ion pair that was constrained from undergoing back-electron transfer ( $k_{BET}$ ). The rate constant for the cleavage of the pinacol cation radical in the inactive ion pair was taken to be the same as that in the contact pair (i.e.,  $k_C$ ). The sum  $k_C$  and  $k_S$  was kept constant at  $1.4 \times 10^{10} \text{ s}^{-1}$  to agree with the experimentally observed quantum yield for the formation of  $MV^{+\bullet}$  (0.3). The simulation generated the family of working curves shown in Figure 4 which represented the

rise of the radical ( $D^*$ ). All of the rises simulated with  $k_S > 0$  showed a distinct time lag between the rise and decay of  $MV^{+\bullet}$  (see Figure 3) and the formation of  $D^*$ . Since the experimental results (dots) showed no time lag and lay on the curve corresponding to  $k_S = 0.0$ , we readily concluded that the “separation” process was not significant on this time scale. The maximum value of  $k_S$  estimated from the error in the datapoints (10%) is about  $1 \times 10^9 \text{ s}^{-1}$ .

The relative amounts of the various transients were determined by comparing their absorbances and quantifying them by using the following extinction coefficients  $\epsilon_{\text{max}} (\lambda_{\text{max}})$ :  $MV^{+\bullet}$ ,  $14100 \text{ M}^{-1} \text{ cm}^{-1}$  (605 nm);<sup>7</sup> diphenylhydroxymethyl (ketyl radical),  $5800 \text{ M}^{-1} \text{ cm}^{-1}$  (535 nm).<sup>14</sup> A value of  $\epsilon_{\text{max}} = 10000 \text{ M}^{-1} \text{ cm}^{-1}$  was used for the biphenyl-substituted pinacol cation radical in accord with the value for biphenyl cation radical.<sup>8</sup>

**Acknowledgment.** We thank the National Science Foundation and the R. A. Welch Foundation for financial support.

JA980097D